

Estimation Bending Deflection in an Ionic Polymer Metal Composite (IPMC) Material using an Artificial Neural Network Model

Bahaa Kazem^{a*}, Jasim Khawwaf^b

^a Mechatronics Engineering Dept., Baghdad University, IRAQ, Visiting Prof., UM-Columbia -USA.

^b Mechatronics Engineering Dept., University of Kufa-IRAQ

Received 30 April 2015

Accepted 15 April 2016

Abstract

The IPMC bending characteristic depends on the accuracy of the manufacturing process for an IPMC specimen and the working conditions such as humidity, temperature, and applied electrical field. So, IPMC behavior is significantly nonlinear and uncertain.

In the present paper, we propose an accurate nonlinear neural Network Black-Box Model (NBBM) to predict the bending motion of IPMC taking into consideration the applied electrical voltage characteristics and the working conditions (specimen dimensions, temperature and humidity of working environment).

An experimental setup and testing program is used to test several IPMC specimens and measure the bending motion at different working conditions and applying electrical voltage signals. The NBBM for the IPMC is designed with suitable input and output parameters to estimate the IPMC specimen tip deflection. The Optimal Brain Surgeon (OBS) pruning algorithm is used to capture the optimal network size and to solve the overfitting problem among the training patterns.

Modeling results show that the optimized NBBM model can best describe the bending behavior of the IPMC specimen according to the applied electrical power signal and the working environment without using any measuring sensor and the proposed model can be used for modeling and controlling the IPMC bending motion in a single segment form.

© 2016 Jordan Journal of Mechanical and Industrial Engineering. All rights reserved

Keywords: IPMC, ANN and Bending.

1. Introduction

In the interest of finding advanced material for modern life, ionic polymer metal composite is an electro-active polymer that is gaining great importance as both a sensor and actuator. A typical Ionic Polymer Metal Composite (IPMC) sheet is a thin ionic polymer membrane (Nafion or Flemion) covered on both sides by two metallic layers (typically gold or platinum) to form two electrodes. When a low electrical field is applied, the transport of hydration cations within the IPMC and the associated electrostatic interactions lead to bending motions of the IPMC sheet toward the anode (+). The cations are initially bound to the anionic groups in the neutral state, forming clusters with the solvent molecules that can easily be exchanged with other cation forms [1].

IPMC has been receiving more and more attention, especially for micro-application. Because of the low driven voltage, flexible operation, large bending, and low weight, IPMC material has been widely applied in many micro-

applications such as snake robots, fish robots, walking robots, and micropumps [1-2].

The IPMC actuation systems exhibit significant nonlinearities and uncertainties. The nonlinearities are mainly caused by the IPMC characteristics during operation. The uncertainties can originate from the external working environment including perturbations and frequency dependent upon the complex elastic modulus E* [3]. These problems cause challenges for modeling the IPMC actuators.

The IPMC characteristic variants depend largely on the working conditions which can lead to oscillations and instabilities in IPMC system performances, especially in applications that require high precision [4-5]. Therefore, it is very useful to investigate the IPMC behaviors for building and simulating an IPMC actuator before applying to practice [6-7].

There are several models available to describe tip displacement of an IPMC. For instance, Newbury and Leo [8] proposed a linear model with mechanical terms, mechanical impedance and inertia, and two electric terms, DC resistance and charge storage. The model was based on

* Corresponding author e-mail: kazemb@missouri.edu.

an equivalent circuit representation that was related to the mechanical, electrical and electromechanical properties of the material. Expressions for the quasi-static and dynamic mechanical impedance were derived from beam theory. The electrical impedance was modeled as a series combination of resistive and capacitive elements. The resulting linear electromechanical model is based on the measurement of the effective permittivity, elastic modulus, and effective strain coefficient. All input-output relationships related to sensing and actuation can be derived using these three material parameters and the transducer geometry.

There are more lumped models available. In those models input parameters such as voltage or current are converted to the output parameters - tip displacement, force, and etc. For instance, Jung and Choi modeled an IPMC as a high pass filter, using series of resistors and capacitors in their calculations [9]. The model was an equivalent electrical circuit model for the IPMC actuator using experimental data.

Punning proposed a non-linear transmission line model, where all the elements of a transmission line had a physical meaning [10]. He showed that the IPMC model works as a delay line with changing resistors and the curvature of the IPMC sample at a given point depends on the surface resistance.

There are few Finite Element models for an IPMC available. Some authors, like Nasser *et al.* [11] and Wallmersperger *et al.* [12], have already simulated mass transfer and electrostatic effects, a similar approach is used in this work. Toi and Kang [13] proposed a Finite Element model, where viscosity terms in transportation processes were included explicitly. However, the basis of the described model was a rectangular beam with 2 pairs of electrodes. Instead of using continuum mechanical equations for simulating mechanical bending, analytical Euler beam theory is more commonly used by authors like Lee [14] and Wallmersperger [15].

Linear and nonlinear black-box models have been identified from experimental data for Ionic Polymer-Polymer Composite (IP2C) actuators had been developed by Graziani [16]. The models take into account the dependence of IP2C actuators behavior on environmental temperature and humidity as relevant modifying inputs.

In order to avoid difficult problems in control, a controller based Adaptive Neuro-Fuzzy Inference System (ANFIS) had been proposed by Thinh *et al.* [17]; it combines the merits of fuzzy logic and neural network, is used for tracking position of IPMC actuator. The results showed that ANFIS algorithm is reliable in controlling IPMC actuator. In addition, experimental results show that the ANFIS performed better than the Pure Fuzzy Controller (PFC). The results show that the proposed adaptive neuro-fuzzy controller can be successfully applied to the real-time control of the ionic polymer metal composite actuator for which the performance degrades under long-term actuation.

Nam & Ahn [18] developed a Nonlinear Black-Box Model (NBBM) for IPMC actuators based on a novel Preisach type fuzzy Nonlinear Auto Regressive Exogenous (NARX) model and modified Particle Swarm Optimization

(PSO). Firstly, an IPMC actuator is investigated. The open-loop input voltage signals are applied to the IPMC in order to investigate the IPMC characteristics. Secondly, a proper Preisach type fuzzy NARX model is developed with one input and one output to estimate the IPMC tip displacement. Modeling results proved the ability of proposed scheme to estimate the bending behaviors of IPMC actuators.

An accurate Nonlinear Black-Box Model (NBBM) for estimating the bending behavior of IPMC actuators had been proposed by Truong and Ahn [19]. The model is constructed via a General Multilayer Perceptron Neural Network (GMLPNN) integrated with a Smart Learning Mechanism (SLM) that is based on an extended Kalman filter with self-decoupling ability (SDEKF). Here the GMLPNN is built with an ability to auto-adjust its structure based on its characteristic vector. Furthermore, by using the SLM based on the SDEKF, the GMLPNN parameters are optimized with small computational effort, and the modeling accuracy is improved. The advanced NBBM model for the IPMC system is created with the proper inputs to estimate IPMC tip displacement. Then the model is optimized using the SLM mechanism with the training data.

A Nonlinear Black-Box Model (NBBM) for IPMC actuators with self-sensing behavior based on a Recurrent Multi-Layer Perceptron Neural Network (RMLPNN) and a Self-Adjustable Learning Mechanism (SALM) had been proposed by Truong *et al.* [20].

Firstly, an IPMC actuator is investigated. Driving voltage signals are applied to the IPMC in order to identify the IPMC characteristics. Secondly, the advanced NBBM for the IPMC is built with suitable inputs and output to estimate the IPMC tip displacement. Finally, the model parameters are optimized by the collected input/output training data.

Modeling results show that the proposed self-sensing methodology based on the optimized NBBM model can well describe the bending behavior of the IPMC actuator corresponding to its applied power without using any measuring sensor.

According to previous researches, understanding IPMC (and smart material in general) characterizations and solving relevant problems are quite difficult tasks because of their complex behavior, which sometimes cannot be identified without intelligent, numerical, and analytical approaches. Because of that, some prediction technique, like Artificial Neural Networks (ANN) can be utilized to solve these problems.

Also, the change in working conditions affects the IPMC characteristics, because it changes the Young modulus and ions density, hence, their mechanical response.

In this work we developed a Nonlinear Black-Box Model (NBBM) based on a Multi-Layer Perceptron Neural Network (MLPNN) to estimate the IPMC tip bending deflection, corresponding to input parameters (electrical voltage amplitude and frequency, temperature and humidity of environment, and dimensions of IPMC (length, and width)) without any measuring sensor.

2. Experimental Setup

In this section, the experimental set-up is described to show the measurement technique for IPMC strip tip motion due to different types of electrical excitation.

The IPMC specimens used in this research were manufactured by Environmental Robots Inc, and can work in both wet and dry environments. The specifications dimensions of the IPMC specimens are shown in Table 1.

Experiments were performed to measure the tip motion of the specimen in the atmosphere. The tip deflection (displacement) was measured at the strip tip as shown in Figure 1. The measurements of displacement were performed under 100–250 mv and 0.07–0.25 Hz square wave. The tip deflection of the IPMC specimen was measured by using a digital camera when the IPMC specimen reached a steady state as shown in Figure 1. It should be noted that there is an accurate relation between each difference in pixels and the real size of difference in the real world. This relationship between specimen image pixels and the actual value of motion is calibrated each time that the recording conditions change. Certainly (as expected), the accuracy is related to the resolution of the camera and distance of the IPMC actuator from the camera. This idea is not new, a similar system has been reported by literatures [21-22].

The environment humidity and temperature were measured using digital instruments. For the experimental tests, the input voltage and frequency are generated by a driving circuit and are measured directly by a digital storage oscilloscope.

The deflections of two different IPMC strips were measured under five different DC voltages and four frequencies of square wave as shown in Tables 2 and 3. The deflections of IPMC strips follow the change of the input voltage well. Figure 2 shows the deflections of the IPMC strips under a square wave. It is expected that high applied voltage and lower frequency results in larger deflection. As the applied voltage increased, the IPMC strip bending deflections for the longer specimen case clearly increased while that for the shorter specimen case slightly increased as expected due to length differences.

Figure 3 shows the variations of the IPMC tip displacement according to the change of applied electrical voltage and the nonlinear behavior for bending behavior for both IPMC strips can be noticed.

The IPMC strips were tested under a voltage range (100 -250) mv square wave form and a frequencies range (0.07-0.25) Hz. Figures 4 and 5 show the maximum bending deflection related with applied frequency for the tested IPMC specimens. The maximum bending deflection becomes larger as the frequency gets smaller and the specimen length becomes longer, the tip deflection of the IPMC specimen change nonlinearly according to the change in frequency of the applied electrical control signals.

3. IPMC Deflection Measurement

Using MATLAB the specimen tip position is calculated for each test setting as listed in Table 2 and 3.

Table 1. Specifications of the IPMC Specimens used in this work

Properties	Ranges	
Electrode and Cations	Platinum and Na ⁺	
Operation environment	Dry/Wet environment -	
Suitable working frequency range	0.05 – 0.25 Hz	
Thickness, Length, Width (mm)	Specimen No.1	Specimen No.2
	0.2,40 ,10	0.2, 30, 5

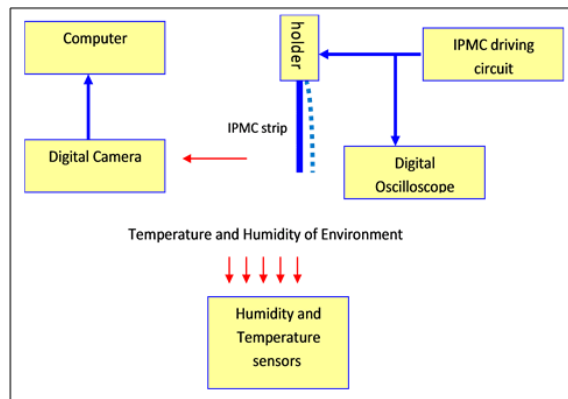


Figure 1. The Block Diagram for Experimental for IPMC actuator



Figure 2. The deflections of the IPMC strips under a square wave, Specimen No. one

Table 2. Data sets generated from IPMC specimen No. one

Pattern No.	Input Voltage (mv)	Frequency of Input(Hz)	Humidity of environment	Temperature of environment (C)	Length of IPMC (mm)	Width of IPMC (mm)	Deflection of IPMC (mm) (Tip displacement)
1	100	0.07	42	22	40	10	4.865
2	100	0.1	42	22	40	10	2.354
3	100	0.15	42	22	40	10	1.4705
4	100	0.25	42	22	40	10	1.4565
5	120	0.07	41	20	40	10	5.4411
6	120	0.1	41	20	40	10	3.088
7	120	0.15	41	20	40	10	1.9115
8	120	0.25	41	20	40	10	1.764
9	155	0.07	32	21	40	10	6.4705
10	155	0.1	32	21	40	10	3.821
11	155	0.15	32	21	40	10	2.352
12	155	0.25	32	21	40	10	2.2058
13	200	0.07	39	22	40	10	7.588
14	200	0.1	39	22	40	10	5.578
15	200	0.15	39	22	40	10	3.382
16	200	0.25	39	22	40	10	2.941
17	250	0.07	40	21	40	10	10.882
18	250	0.1	40	21	40	10	7.351
19	250	0.15	40	21	40	10	5.589
20	250	0.25	40	21	40	10	4.558

Table 3. Data sets generated from IPMC specimen No. two

Pattern No.	Input Voltage (mv)	Frequency of Input(Hz)	Humidity of environment	Temperature of environment (C)	Length of IPMC (mm)	Width of IPMC (mm)	Deflection of IPMC (mm) (Tip displacement)
1	100	0.07	38	22	30	5	2.94
2	100	0.1	38	22	30	5	1.465
3	100	0.15	38	22	30	5	.5605
4	100	0.25	38	22	30	5	.294
5	120	0.07	40	22	30	5	3.167
6	120	0.1	40	22	30	5	1.473
7	120	0.15	40	22	30	5	.9725
8	120	0.25	40	22	30	5	.441
9	155	0.07	36	21	30	5	3.821
10	155	0.1	36	21	30	5	2.2058
11	155	0.15	36	21	30	5	1.3945
12	155	0.25	36	21	30	5	.458
13	200	0.07	40	23	30	5	4.85
14	200	0.1	40	23	30	5	2.647
15	200	0.15	40	23	30	5	1.4708
16	200	0.25	40	23	30	5	.538
17	250	0.07	40	21	30	5	6.175
18	250	0.1	40	21	30	5	3.088
19	250	0.15	40	21	30	5	1.5961
20	250	0.25	40	21	30	5	1.029

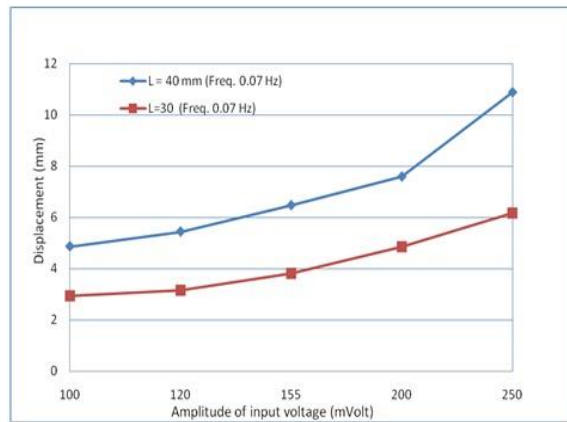


Figure 3. Maximum IPMC bending deflection with respect to the input voltage

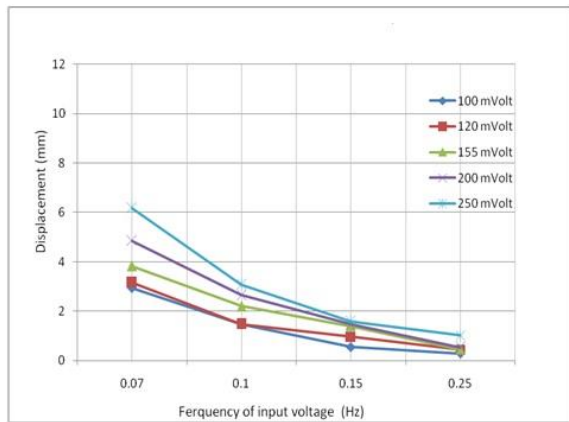


Figure 4. Maximum IPMC Tip Deflection change according to the change in applied Electrical Voltage Amplitude and Frequency for specimen of length 30 mm

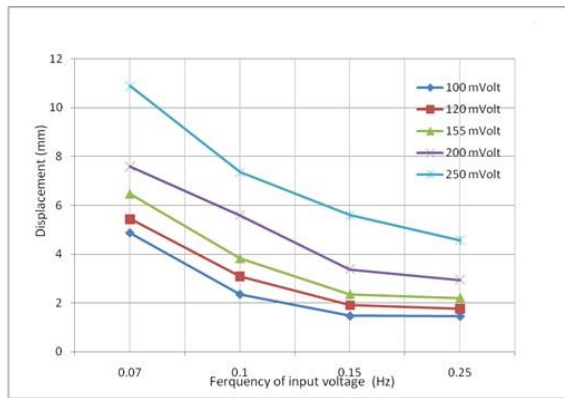


Figure 5. Maximum Tip Deflection change according to the change in applied Electrical Voltage Amplitude and Frequency for specimen of length 40 mm

4. A Nonlinear Black-Box Model for IPMC Actuator (NBBM)

A neural network can be defined as a model of reasoning based on the human brain. The brain consists of a densely interconnected set of nerve cells, or basic information processing units, called neurons [23].

Neural networks are composed of simple elements operating in parallel. As in nature, the network function is determined largely by the connections between elements. You can train a neural network to perform a particular function by adjusting the values of the connections (weights) between elements. Commonly neural networks are adjusted, or trained, so that a particular input leads to a specific target output. Such a situation can be shown as follows: there, the network is adjusted, based on a comparison of the output and the target, until the network output matches the target. Typically many such input/target pairs are needed to train a network[24], [25].

One of the advantages of neural networks is its ability to model nonlinear problems those are hard to solve mathematically. Neural network can deal with any problems that can be represented as patterns.

Therefore, to solve the difficulty of IPMC modeling, we will use a nonlinear black-box model, which contain Multi-Layer Perceptron Neural Network (MLPNN) as a nonlinear model, is designed to model highly nonlinear systems in general and the IPMC actuator in particular.

A feed forward neural network distinguishes itself by the presence of one or more hidden layers, whose computation nodes are correspondingly called hidden neurons or hidden units, Figure 6. The function of hidden neurons is to intervene between the external input and the network output in some useful manner. By adding one or more hidden layers, the network is enabling to extract higher order statistics.

Multi-layer feed forward networks commonly referred as (MLP) are an important class of neural networks. MLPs have been applied successfully to solve some difficult and diverse problems in many disciplines of science and technology. The main method of training MLPs is the error back propagation, which was recognized several groups of scientists [26]–[30]

MLP is supervised network so it requires a desired response to be trained. With one or more hidden layers,

they can approximate virtually any input-output map. Figure 6 shows a typical network structure [20] which contains an input layer (on the left) with n neurons, k hidden layers (in the middle) of which the j^{th} layer contains q_j neurons, and an output layer (on the right) with m neurons .The input layer is represented by a vector of input variables (u_1, \dots, u_n). the input layer distributes these values to each of the neurons in the first hidden layer. At each neuron in a hidden layer, the output values from its previous layer are multiplied by weights (w), and the resulting weight values are added together, producing a combined value (sh_j) as given at Equation 1:

$$sh_i = \sum_{i=1}^n w_{ij} u_i, \quad j = 1, \dots, q_1 \quad (1)$$

for each node in the 1st hidden layer

$$sh_i = \sum_{i=1}^{ql-1} w_{ij} o h_i + w_{j0} o h_{l-1}, \quad j = 1, \dots, q_1 \quad (1)$$

for each node in the lth hidden layer

where sh is the weighted sum, also there are a series of constants from b_0 to b_k , which are called ‘bias’ factors, that are fed to the input layer and each of the hidden layers. The weighted sum (sh) is then fed into a transfer function, F , to obtain the outputs a value of neuron j^{th} (oh). The outputs from the final hidden layer are distributed to the output layer.

At neuron, p^{th} in the output layer, output values from the final hidden layer neurons are multiplied by weights (W) and added together to produce a combined value (sh). This sum is fed into a transfer function, F , to compute the outputs value of neuron $p^{\text{th}}(oh)$.this value is then, gained with a suitable factor to a corresponding output (y). The values y are the outputs of the network.

For hidden as well as output units, sigmoid activation functions are usually preferable to threshold activation functions. Networks with threshold units are difficult to train because the error function is stepwise constant. In this work, we used the Levenberg-Marquard training algorithm in addition to Gradient Descent with Momentum algorithm and Conjugate Gradient Descent algorithm. For sigmoid units, a small change in the weights usually produces a change in the outputs, which makes it possible to tell whether that change in the weights is good or bad. The designed MLPNN structure in this research is built with sigmoid activation functions given in equation 2.

Hence, the output of each hidden node can be computed using Equation 2:

$$oh_j = F(sh_j) = \frac{1}{1 + e^{-sh_j}} \quad (2)$$

From Equation 2, it is clear that the output oh closes to the boundaries 0 and 1. In the present study, we normalize the inputs in the range $[+1, -1]$. Each of the outputs in the output layer can be obtained as Equation 3:

$$\hat{y} = k_p \times oh_p \quad (3)$$

where k_p is a scaling gain corresponding to output p^{th} selected from the output range.

$$\left\{ \begin{array}{l} oh_p = F(sh_p) = \frac{1}{1 + e^{-sh_p}} \\ sh_p = \left(\sum_{j=1}^{qk} W_j oh_j + W_o b_k \right) \end{array} \right. \quad (4)$$

$$sh_p = \left(\sum_{j=1}^{qk} W_j oh_j + W_o b_k \right) \quad p = 1, \dots, m \quad (5)$$

The NBBM model possessed both the powerful universal approximating features from the MLPNN structure. Different structures of MLPNN related to training algorithm and hidden layers have been investigated in order to obtain the optimized neural network model for estimate the IPMC tip deflection.

It is well known that the model structure as well as the training algorithm is very important in the selection model of a neural network. Since there is a large number of training algorithms for feed forward neural network, one cannot easily decide which performs better for a specific application. Thus the neural network model was trained using three different training algorithms:

1. Gradient Descent with Momentum algorithm
2. Levenberg – Marquardt algorithm
3. Conjugate Gradient Descent algorithm

Also, we used two different activation functions in output layer:

1. Linear activation function
2. Log sigmoid activation function

The performances of these three training algorithms were tested using different types of activation functions and compared with each other to decide best algorithm that able to capture IPMC behavior. We randomly selected 80% of the total patterns to train the networks. Once a neural network has been trained successfully using MATLAB®, it can perform the required mappings as a sort of black box. To check the ability of the network to deal with new patterns which are similar to learned patterns (generalization of the network), we used the remaining 10% of the patterns for validation and 10% for testing of the performance of the network.

Table 4 shows the correlation values for the results of the training, and testing results using different training algorithms and different activation functions after 1000 iterations. The selection of the best network will based on which hidden unit gives the lowest testing Error results. The network error (Train Error and Test Error) is calculated as the sum of the squared differences between the actual value (target value) and neural network output.

After examining the performance of different structures with different training algorithms, a network with more than 10 hidden neurons trained by Levenberg-Marquardt algorithm and log sigmoid activation function for output layer showed good performance indices as shown in Figure 7.

Despite many advances, for neural network to find general applicability in real world problems, the crucial question is to determine the most appropriate network size for solving a specific task. The network designer dilemma stems from the fact that both large and small networks exhibit a number of shortcomings. When the network has

too many degrees of freedom (network weights and biases), more local minima, instead of reaching global minima, in addition to the overfitting problem among training patterns makes the network fail to generalize its knowledge acquired during training phase. To solve the problem of choosing the optimal size network, an Optimal Brain Surgeon (OBS) pruning algorithm is used. The aim of an OBS pruning algorithm is to capture the optimal network size by gradually reducing (a large trained) network's degrees of freedom. The algorithm is based on the idea of iteratively removing a single degree of freedom (weight or bias) and then adjusting the remaining weight with a view to maintaining the original input – output behavior [31]-[33].

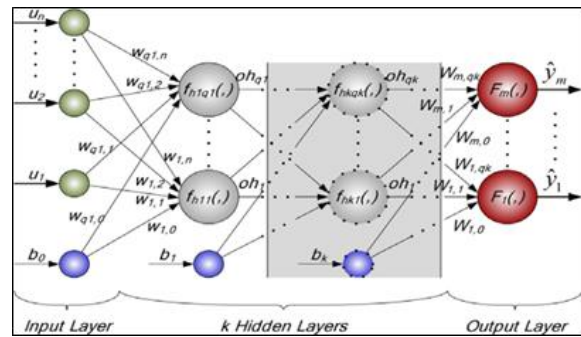


Figure 6. Structure of a Feed Forward MLPNN system [20]

5. Modeling Results

The major advantage of neural network predictions is that the model can estimate the IPMC tip deflection accurately once input variables (voltage, frequency, length and width of IPMC, and temperature and humidity of environment) are known.

The developed neural network model is used to estimate the IPMC tip deflection of the available training patterns which show a reasonable agreement between the target and the estimated values as illustrated in Figure 8. From this figure, it is clear that the optimized NBBM model can estimate the IPMC tip deflection with high precision and then be able to be applied to IPMC control system as a "virtual tip deflection sensor" for the self-sensing behavior.

The neural network model can give insight about the effect of each input variables (voltage, frequency, length and width of IPMC, temperature and humidity of environment) on the estimation of the IPMC tip displacement. The effect each of input variable is shown in Table 5. Thus, the temperature and humidity show very limited effect on the proposed NBBM model predication and can be neglected in practical implementation of the model. The estimated results for the effectiveness of each working-variable on the IPMC tip displacement is highly depended on the working variables ranges and need to repeat the training for any new set of working variables and IPMC specimens.

Table 4. Correlation between training error and testing error for deferent neural networks training algorithm and activation function type

No. of hidden neurons	Correlation value					
	Gradient Descent activation function of output layer log sigmoid	Gradient Descent activation function of output layer linear	Levenberg – Marquardt Algorithm activation function of output layer log sigmoid	Levenberg – Marquardt Algorithm activation function of output layer linear	Conjugate Gradient Descent activation function of output layer log sigmoid	Conjugate Gradient Descent activation function of output layer linear
5	0.802599	0.994411	0.938098	0.788558	0.624325	0.962059
6	0.763727	0.744328	0.916023	0.940821	0.644214	0.986909
7	0.819456	0.751879	0.991105	0.489284	0.705154	0.632704
8	0.844334	0.709663	0.992142	0.959573	0.662197	0.613903
9	0.826479	0.725508	0.925715	0.676961	0.804905	0.609026
10	0.810121	0.710661	0.995163	0.85257	0.670168	0.622467
11	0.837673	0.703325	0.998624	0.934037	0.953935	0.648482
12	0.804059	0.665097	0.993454	0.999425	0.668997	0.999909
13	0.835637	0.658603	0.904077	0.994023	0.627829	0.705363
14	0.820606	0.658175	0.999982	0.999772	0.996477	0.582949
15	0.800279	0.724997	0.994709	0.961663	0.65892	0.619741

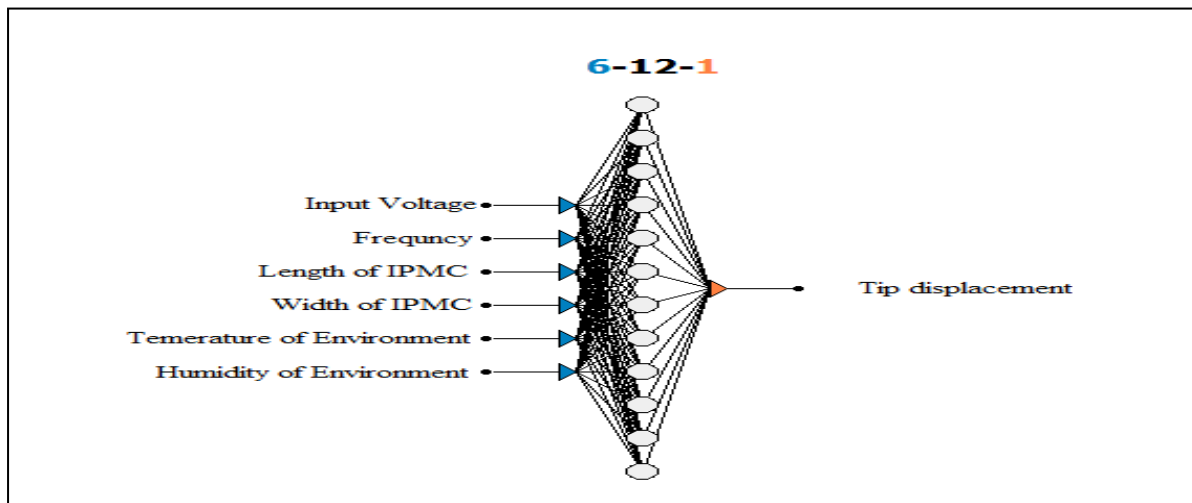
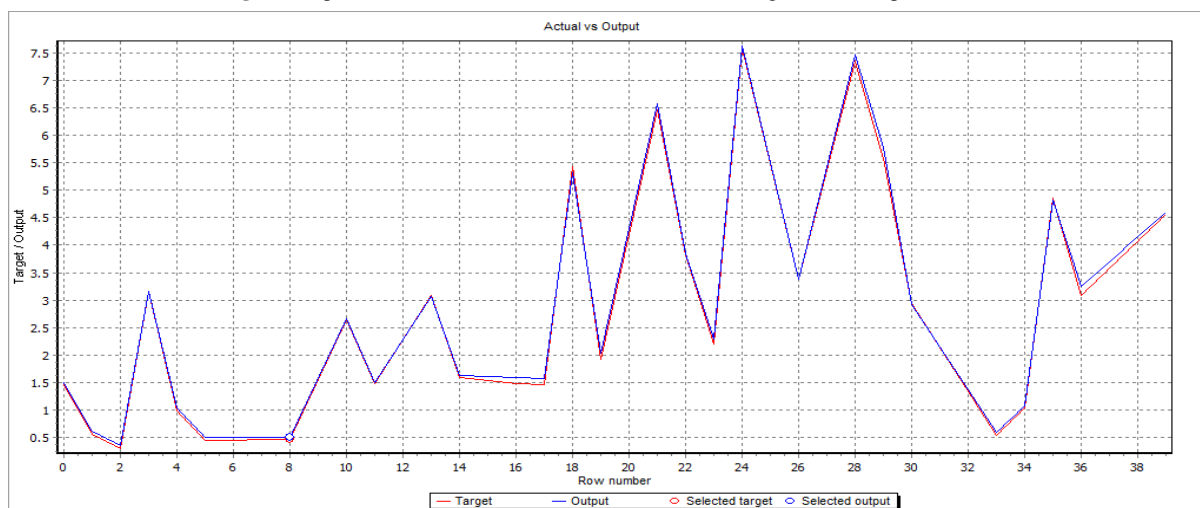
**Figure 7.** Optimized Neural Network Architecture for estimating the IPMC Tip Deflection**Figure 8 .**The IPMC Tip Deflection using the Proposed Neural Network Model

Table 5. The estimated effects of working-variables on IPMC tip displacement as they predicted by NBBM

working variable	Percentage effect on IPMC Displacement (%)
Voltage (mv)	24.577515
Frequency (Hz)	29.769568
Length of IPMC (mm)	18.294952
Width of IPMC (mm)	18.492071
Temperature of Environment (C°)	5.799173
Humidity of Environment (dry/ wet)	3.066722

6. Conclusions

In this work we presented a Nonlinear Black-Box Model (NBBM) to estimate IPMC deflection response, the model is based on the multi-layer perception neural network. The results show that the model can well describe the IPMC Tip deflection, corresponding to operation variables for IPMC actuator (Input voltage, frequency, dimensions of length of IPMC, temperature and humidity of environment).

After examining the performance of the suggested neural networks structures, a neural network with 12 hidden neurons trained by the Levenberg-Marquardt algorithm, and using log sigmoid activation function, showed good performance indices.

The proposed NBBM model takes into account the dependence of IP2C actuators behavior on environmental temperature and humidity as relevant modifying inputs.

References

- [1] M. Lopez, B. Kipling, and H. L. Yeager, "Ionic diffusion and selectivity of a cation exchange membrane in nonaqueous solvents," *Anal. Chem.*, Vol. 49 (1977) No. 4, 629–632.
- [2] K. J. Kim and S. Tadokoro, Eds., *Electroactive Polymers for Robotic Applications*. London: Springer London, 2007.
- [3] S. J. Lee, M. J. Han, S. J. Kim, J. Y. Jho, H. Y. Lee, and Y. H. Kim, "A new fabrication method for IPMC actuators and application to artificial fingers," *Smart Mater. Struct.*, Vol. 15 (2006) No. 5, 1217–1224.
- [4] C. Bonomo, P. Brunetto, L. Fortuna, P. Giannone, S. Graziani, and S. Strazzeri, "A Tactile Sensor for Biomedical Applications Based on IPMCs," *IEEE Sens. J.*, Vol. 8 (2008) No. 8, 1486–1493.
- [5] H. Jung and D.-G. Gweon, "Creep characteristics of piezoelectric actuators," *Rev. Sci. Instrum.*, Vol. 71 (2000) No. 4, 1896.
- [6] K. Tsiaimakis, J. Brufau, M. Puig-Vidal, and T. Laopoulos, "Modeling IPMC Actuators for Model Reference Motion Control", *2008 IEEE Instrumentation and Measurement Technology Conference*, 2008, pp. 1168–1173.
- [7] Z. Chen, L. Hao, D. Xue, X. Xu, and Y. Liu, "Modeling and control with hysteresis and creep of ionic polymer-metal composite (IPMC) actuators", *2008 Chinese Control and Decision Conference*, 2008, pp. 865–870.
- [8] K. M. NEWBURY and D. J. LEO, "Linear Electromechanical Model of Ionic Polymer Transducers -Part I: Model Development," *J. Intell. Mater. Syst. Struct.*, Vol. 14 (2003) No. 6, 333–342 2003.
- [9] K. Jung, J. Nam, and H. Choi, "Investigations on actuation characteristics of IPMC artificial muscle actuator," *Sensors Actuators A Phys.*, Vol. 107 (2003) No. 2, 183–192.
- [10] A. Punning, M. Kruusmaa, and A. Aabloo, "Surface resistance experiments with IPMC sensors and actuators," *Sensors Actuators A Phys.*, Vol. 133 (2007) No. 1, 200–209.
- [11] S. Nemat-Nasser and S. Zamani, "Modeling of electrochemomechanical response of ionic polymer-metal composites with various solvents," *J. Appl. Phys.*, Vol. 100 (2006) No. 6, 064310.
- [12] T. Wallmersperger, B. Kröplin, and R. W. Gülich, "Coupled chemo-electro-mechanical formulation for ionic polymer gels—numerical and experimental investigations," *Mech. Mater.*, Vol. 36 (2004) No. 5–6, 411–420.
- [13] Y. Toi and S.-S. Kang, "Finite element analysis of two-dimensional electrochemical–mechanical response of ionic conducting polymer–metal composite beams," *Comput. Struct.*, Vol. 83 (2005) No. 31–32, 2573–2583.
- [14] S. Lee, H. C. Park, and K. J. Kim, "Equivalent modeling for ionic polymer–metal composite actuators based on beam theories," *Smart Mater. Struct.*, Vol. 14 (2005) No. 6, 1363–1368.
- [15] T. Wallmersperger, D. J. Leo, and C. S. Kothera, "Transport modeling in ionomeric polymer transducers and its relationship to electromechanical coupling," *J. Appl. Phys.*, Vol. 101 (2007) No. 2, 024912.
- [16] S. Graziani, E. Umana, M. G. Xibilia, and V. De Luca, "Multi-input identification of IP2C actuators," in *2013 IEEE International Instrumentation and Measurement Technology Conference (I2MTC)*, 2013, 1147–1151.
- [17] N. T. Thinh, Y.-S. Yang, and I.-K. Oh, "Adaptive neuro-fuzzy control of ionic polymer metal composite actuators," *Smart Mater. Struct.*, Vol. 18 (2009) No. 6, 065016.
- [18] D. N. C. Nam and K. K. Ahn, "Identification of an ionic polymer metal composite actuator employing Preisach type fuzzy NARX model and Particle Swarm Optimization," *Sensors Actuators A. Phys.*, Vol. 183 (2012), 105–114.
- [19] D. Q. Truong and K. K. Ahn, "Modeling of an ionic polymer metal composite actuator based on an extended Kalman filter trained neural network," *Smart Mater. Struct.*, Vol. 23 (2014) No. 7, 074008.
- [20] D. Q. Truong, K. K. Ahn, D. N. C. Nam, and J. Il Yoon, "Identification of a nonlinear black-box model for a self-sensing polymer metal composite actuator," *Smart Mater. Struct.*, Vol. 19 (2010) No. 8, 085015.
- [21] Y. Bar-Cohen, X. Bao, S. Sherrit, and S.-S. Lih, "Characterization of the electromechanical properties of ionomeric polymer–metal composite (IPMC)," in *SPIE's 9th Annual International Symposium on Smart Structures and Materials*, 2002, pp. 286–293.
- [22] B. C. Lavu, M. P. Schoen, and A. Mahajan, "Adaptive intelligent control of ionic polymer–metal composites," *Smart Mater. Struct.*, Vol. 14 (2005) No. 4, pp. 466–474.
- [23] M. Negnevitsky, *Artificial Intelligence: A Guide to Intelligent Systems*. 3rd Edition: Addison-Wesley 2011.
- [24] E. A. Metzbower, J. J. DeLoach, S. H. Lalam, and H. K. D. H. Bhadeshia, "Secondary effects in neural network analysis of the mechanical properties of welding alloys for HSLA shipbuilding steels," *Math. Model. Weld Phenomena* 6, eds, Cerjak and K. D. H. Bhadeshia, London, p. 231–242, 2002.
- [25] D. M. Eugene Charniak. *Introduction to Artificial Intelligence*. Addison-Wesley Series in Computer Science; 1985.
- [26] C. Vana, Vital Rao; Ratnamb, "Estimation of Defect Severity in Rolling Element Bearings using Vibration Signals with Artificial Neural Network," *Jordan Journal of Mechanical and Industrial Engineering*, Vol. 9 (2015) No.2,113-120.

- [27] B. I. Kazem, N. F.H. Zangana, "A Neural Network Based Real Time Controller for Turning Process," *Jordan Journal of Mechanical and Industrial Engineering*, Vol. 1 (2007) No. 1, 43-55..
- [28] N. Ashhab, M; Talatb, "Modeling of the MEMS Reactive Ion Etching Process Using Neural Networks," *Jordan Journal of Mechanical and Industrial Engineering*, Vol. 5 (2011) No. 4, 353 - 357.
- [29] B. I. Kazem. YK Yousif, KM Daws, "Prediction of Friction Stir Welding Characteristic Using Neural Network," *Jordan Journal of Mechanical and Industrial Engineering*, Vol. 2 (2008) No. 3, 151-155.
- [30] B. I. Kazem, N. H. Ghaib, and N. M. H. Grama, "Experimental Investigation and Neural Network Modeling for Force System of Retraction T-Spring for Orthodontic Treatment," *J. Med. Device.*, Vol. 4 (2010) No. 2,021001.
- [31] M. Hintz-Madsen, L. Kai Hansen, J. Larsen, M. With Pedersen, and M. Larsen, "Neural classifier construction using regularization, pruning and test error estimation," *Neural Networks*, Vol. 11 (1998) No. 9, 1659–1670.
- [32] G. Castellano, A. M. Fanelli, and M. Pelillo, "An iterative pruning algorithm for feedforward neural networks., " *IEEE Trans. Neural Netw.*, Vol. 8 (1997) No. 3, 519–31.
- [33] B. I. Kazem, Ali Khudhair Mutlag, "Optimal Brain Surgeon Pruning of Neural Network Models of Manufacturing Processes" , *Journal of Engineering*, Vol. 11 (2005) No. 3, 495-508.